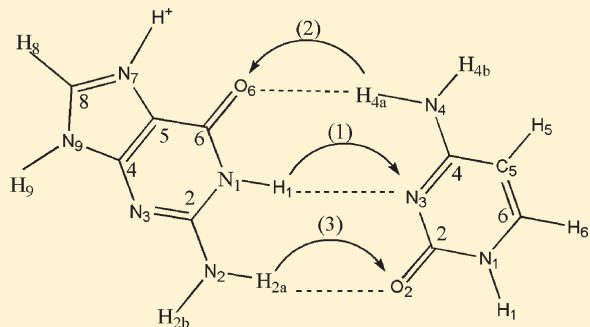


Hydrogen-Bonded Proton Transfer in the Protonated Guanine-Cytosine (GC+H)⁺ Base Pair

Yuxia Lin,[†] Hongyan Wang,^{*,†} Simin Gao,[†] and Henry F. Schaefer, III[‡][†]School of Physical Science and Technology, Southwest Jiaotong University, Chengdu 610031, People's Republic of China[‡]Center for Computational Quantum Chemistry, University of Georgia, Athens, Georgia 30602, United States

ABSTRACT: The single proton transfer at the different sites of the Watson–Crick (WC) guanine-cytosine (GC) DNA base pair are studied here using density functional methods. The conventional protonated structures, transition state (TS) and proton-transferred product (PT) structures of every relevant species are optimized. Each transition state and proton-transferred product structure has been compared with the corresponding conventional protonated structure to demonstrate the process of proton transfer and the change of geometrical structures. The relative energies of the protonated tautomers and the proton-transfer energy profiles in gas and solvent are analyzed. The proton-transferred product structure $G(+H^+)-H^+C_{N3^-}(-H^+)_{PT}$ has the lowest relative energy for which only two hydrogen bonds exist. Almost all 14 isomers of the protonated GC base pair involve hydrogen-bonded proton transfer following the three pathways, with the exception of structure $G-H^+C_{O2}$. When the positive charge is primarily “located” on the guanine moiety (H^+G-C , $G-H^+C_{C4}$, and $G-H^+C_{C6}$), the H_1 proton transfers from the N_1 site of guanine to the N_3 site of cytosine. The structures $G-H^+C_{CS}$ and $G-H^+C_{C4}$ involve H_{4a} proton transfer from the N_4 of cytosine to the O_6 site of guanine. H_{2a} proton transfer from the N_2 site of guanine to the O_2 site of cytosine is found only for the structure $G-H^+C_{C4}$. The structures to which a proton is added on the six-centered sites adjoining the hydrogen bonds are more prone to proton transfer in the gas phase, whereas a proton added on the minor groove and the sites adjoining the hydrogen bonds is favorable to the proton transfer in energy in the aqueous phase.



1. INTRODUCTION

Almost 60 years ago Watson and Crick¹ built their double-helix model of the three-dimensional structure of DNA, from which they proposed that nucleic acids and nucleobases play an essential role in the process of DNA replication. Subsequent theoretical and experimental studies of DNA focused on the geometrical structure, energies, and physicochemical characters of the nucleic acids and nucleobases.^{2–17} Hutter and Clark⁵ reported ab initio and density functional calculations on the ionized DNA bases and base pairs in 1996, whose results were in broad agreement with previous theoretical studies^{6,7} and experimental measurements^{8,9} showing that guanine and adenine are the two most easily oxidized bases. Three years later the isomerization and tautomerization energies of the pyrimidine and purine nucleic acid bases and related compounds were predicted by Ha and Keller.¹¹ The following year Podolyan, Gorb, and Leszczynski studied the protonation of all nucleic acid bases using ab initio post-Hartree–Fock levels of theory and obtained their relative stabilities and proton affinities.¹³ Kampf et al. compared the acid–base properties of purine derivatives in aqueous solution and determined the intrinsic proton affinities of various basic sites in 2002.¹⁵ In 2007 Zhang et al. discussed the geometrical structure and energy of the radicals generated by hydrogen-atom addition to the Watson–Crick guanine-cytosine (GC) DNA base pair.¹⁷

DNA damage and repair processes are often caused by electron, hydrogen atom, proton, and hydride migration.^{19–22} Recently, even more scientists have plunged into studies of the mechanism of the proton transfer within nucleic acids and base pairs,^{23–44} which mechanism is considered one factor related to DNA damage and repair due to DNA mutation. Florián and Leszczynski²³ studied the spontaneous DNA mutations induced by proton transfer in GC base pairs. Cerón-Carrasco et al. studied double proton-transfer mechanisms in the adenine-uracil base pair and spontaneous mutation in the RNA duplex. Bertrand²⁵ discussed the differences between electron shift and proton transfer from an experimental perspective, and briefly described related mechanisms. Leszczynski explored double proton-transfer reactions in the AT and GC base pairs at the B3LYP and MP2 levels of theory in 2004.²⁶ The proton-transfer process is influenced by various factors. For the base pairs with disparate moiety charge distributions, through ionization^{33–37} or introduced charged ions,^{28,29,38–40} single proton transfer becomes much easier. Bertran et al.³⁵ studied single vs double proton-transfer reactions in Watson–Crick base pair radical cations using the hybrid density functional B3LYP

Received: June 9, 2011

Revised: September 2, 2011

Published: September 03, 2011

method and showed that single proton-transfer reaction is favorable in both the GC and AT radical cations. Noguera, Sodupe, and Bertrán^{28,38} have explored the $(G)N_1-H\cdots N_3(C)$ proton-transfer process in the GC base pair attached a proton or $Cu^{2+/+}$ with the B3LYP density function. In the real biological situation, DNA mutations are affected by solvation and nucleobase sequence, etc.^{40–44} Nonin et al.⁴⁰ have proposed that acid-induced catalysis can improve the proton-transfer rate. The water molecules around base pairs are favorable to proton transfer.^{24,31,32,41,42} Sevilla and co-workers have studied hydration effects on the proton-transfer mechanism in hydrated base pairs using theory⁴¹ and experiment.⁴² The results suggest that microhydration may play a crucial role for proton-transfer reaction in DNA basis pairs.

Protons are present in environments surrounding base pairs, especially in acid solvents. The proton-transfer process in protonated DNA base pairs is a key point in understanding DNA damage and DNA repair.^{28,29,41} Wang et al. systematically studied the protonated GC base pairs¹⁸ and analyzed the structures and energies of the 14 tautomers of the protonated GC base pairs. In this paper, we investigate the single proton transfer at the different protonated sites of the GC base pair. The geometrical structures and relative energies, hydrogen bonds and natural bond orbital (NBO) charge distributions, as well as the proton-transfer energy profile in gas and solvent, are discussed.

2. THEORETICAL METHODS

The geometries of the proton-transferred products and the transition states associated with proton transfer for the 14 tautomers of protonated GC base pair were fully optimized using the B3LYP density functional. The B3LYP method is a combination of the Becke three-parameter exchange functional (B3)⁴⁵

Scheme 1. Three Possible Hydrogen-Bonded Proton-Transfer Pathways

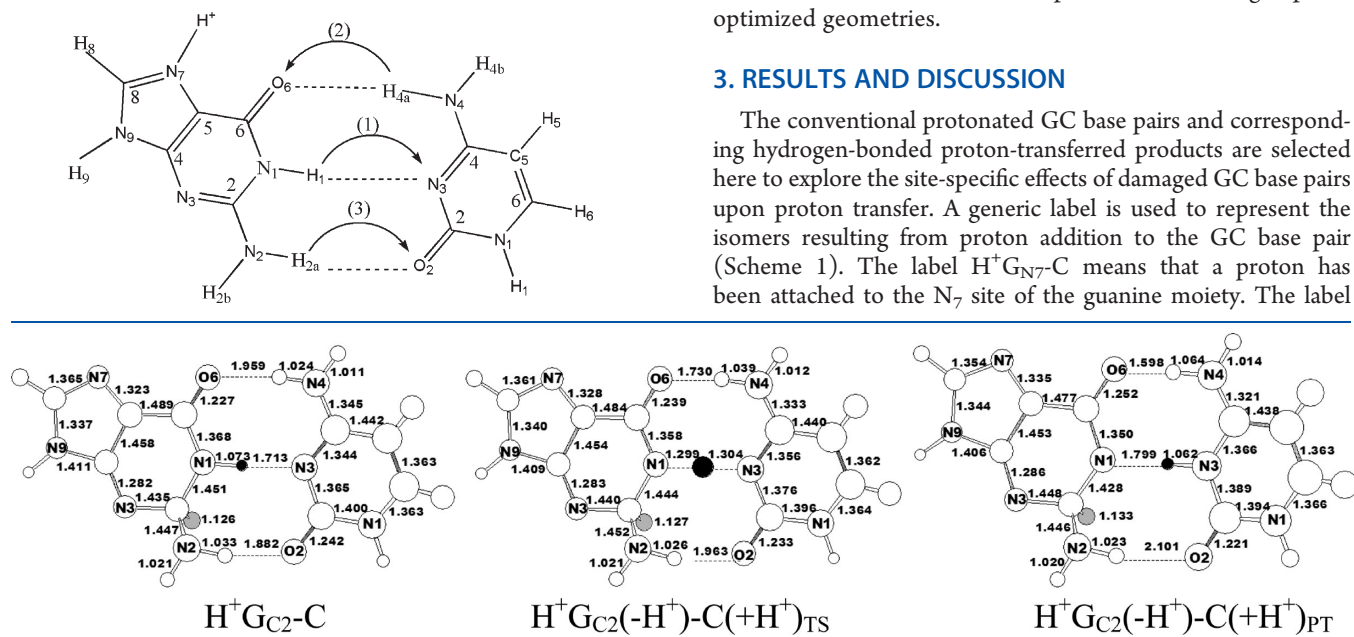


Figure 1. The optimized conventional protonated structure $H^+G_{C2}-C$, transition state (TS) structure $H^+G_{C2}(-H^+)-C(+H^+)_{TS}$, and proton-transferred product (PT) $H^+G_{C2}(-H^+)-C(+H^+)_{PT}$.

and the dynamic correlation functional of Lee, Yang, and Parr (LYP).⁴⁶ Such DFT methods have been used for many studies^{47,48} of hydrogen-bonded systems. These investigations seem to show that nonlocal methods including gradient corrections, particularly B3LYP, provide reliable results. Vibrational frequency analyses were also performed at the same level to ensure the $(GC+H)^+$ are local minima. For the $(GC+H)^+$ structures, a single imaginary vibrational frequency was found. The Gaussian 09⁴⁹ system of DFT program was used for the computations.

Double- ζ quality basis sets with polarization and diffuse functions (DZP++) are used in this research. The DZP++ basis sets were constructed by augmenting the Huzinaga–Dunning^{50,51} set of contracted double- ζ Gaussian functions with one set of p-type polarization functions for each H atom and one set of five d-type polarization functions for each C, N, and O atom [$\alpha_p(H) = 0.75$, $\alpha_d(C) = 0.75$, $\alpha_d(N) = 0.80$, $\alpha_d(O) = 0.85$]. To complete the DZP++ basis, one even-tempered diffuse s function was added to each H atom, while sets of even-tempered diffuse s and p functions were centered on each heavy atom. The even-tempered orbital exponents were determined according to the prescription of Lee⁵²

$$\alpha_{\text{diffuse}} = \frac{1}{2} \left(\frac{\alpha_1}{\alpha_2} + \frac{\alpha_2}{\alpha_3} \right) \alpha_1$$

where α_1 , α_2 , and α_3 are the three smallest Gaussian orbital exponents of the s- or p-type function for a given atom ($\alpha_1 < \alpha_2 < \alpha_3$). The final DZP++ set includes six functions per H atom (5s1p/3s1p) and nineteen functions per C, N, or O atom (10s6p1d/5s3p1d), yielding a total of 427 contracted Gaussian functions for each $(GC+H)^+$ protonated base pair structure. This basis has the tactical advantage that it has previously been used in many successful studies⁵³ of proton affinities.

Solvent effects are assessed through polarizable continuum model (PCM) single-point calculations with the same method and basis set as used for the gas phase species. The influence of water molecules is taken into account by a polarizable continuum. These calculations are performed at the gas phase optimized geometries.

3. RESULTS AND DISCUSSION

The conventional protonated GC base pairs and corresponding hydrogen-bonded proton-transferred products are selected here to explore the site-specific effects of damaged GC base pairs upon proton transfer. A generic label is used to represent the isomers resulting from proton addition to the GC base pair (Scheme 1). The label $H^+G_{N7}-C$ means that a proton has been attached to the N₇ site of the guanine moiety. The label

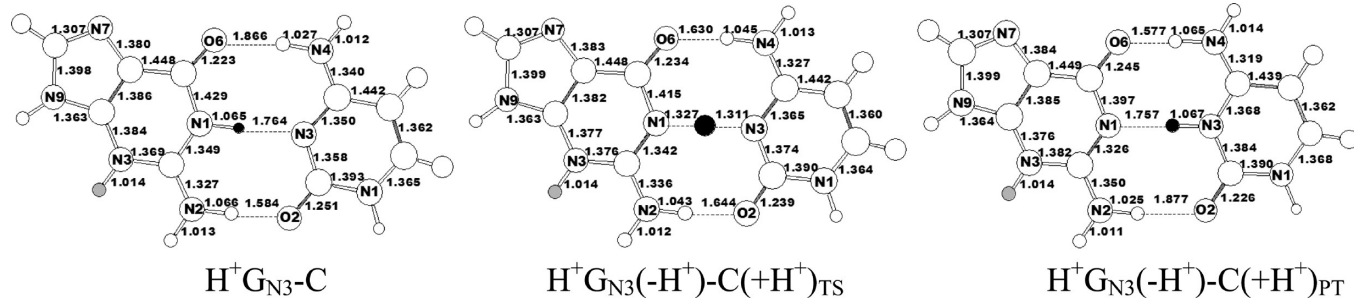


Figure 2. The optimized conventional protonated structure $\text{H}^+\text{G}_{\text{N}3}\text{-C}$, transition state (TS) structure $\text{H}^+\text{G}_{\text{N}3}(\text{-H}^+)\text{-C}(\text{+H}^+)_{\text{TS}}$, and proton-transferred product (PT) $\text{H}^+\text{G}_{\text{N}3}(\text{-H}^+)\text{-C}(\text{+H}^+)_{\text{PT}}$.

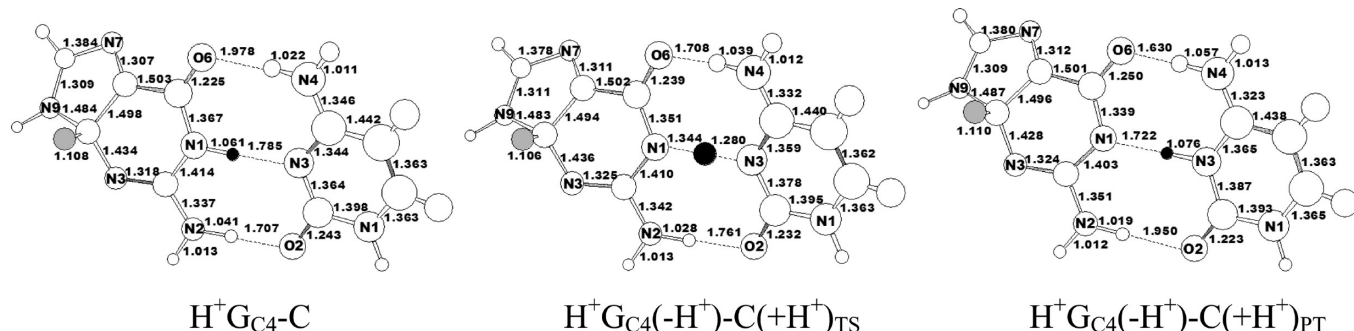


Figure 3. The optimized conventional protonated structure $\text{H}^+\text{G}_{\text{C}4}\text{-C}$, transition state (TS) structure $\text{H}^+\text{G}_{\text{C}4}(\text{-H}^+)\text{-C}(\text{+H}^+)_{\text{TS}}$, and proton-transferred product (PT) $\text{H}^+\text{G}_{\text{C}4}(\text{-H}^+)\text{-C}(\text{+H}^+)_{\text{PT}}$.

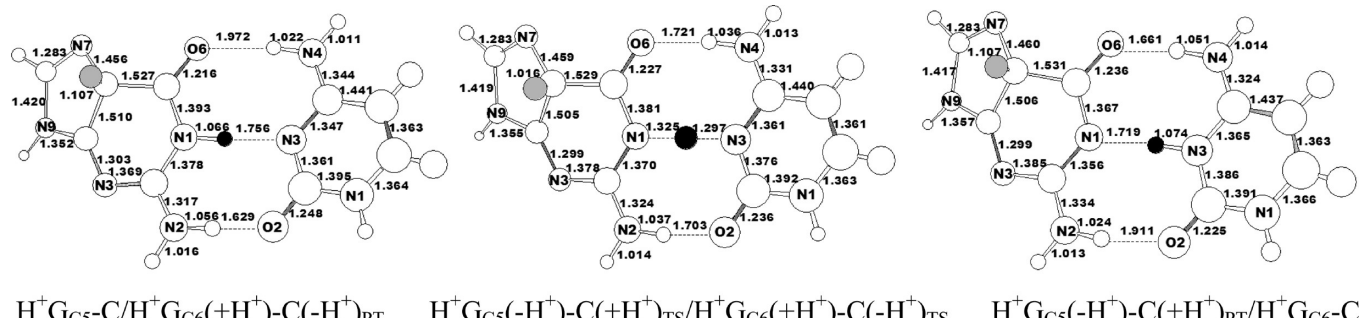


Figure 4. The optimized conventional protonated structures $\text{H}^+\text{G}_{\text{C}5}\text{-C}$ and $\text{H}^+\text{G}_{\text{C}6}\text{-C}$, transition state (TS) structure $\text{H}^+\text{G}_{\text{C}5}(\text{-H}^+)\text{-C}(\text{+H}^+)_{\text{TS}}$ or $\text{H}^+\text{G}_{\text{C}6}(\text{+H}^+)\text{-C}(\text{-H}^+)_{\text{TS}}$, and proton-transferred product (PT) $\text{H}^+\text{G}_{\text{C}5}(\text{-H}^+)\text{-C}(\text{+H}^+)_{\text{PT}}$ or $\text{H}^+\text{G}_{\text{C}6}(\text{+H}^+)\text{-C}(\text{-H}^+)_{\text{PT}}$.

$\text{H}^+\text{G}_{\text{N}7}(\text{-H}^+)\text{-C}(\text{+H}^+)_{\text{TS}}$ means that the transition state of the proton transfer, and $\text{H}^+\text{G}_{\text{N}7}(\text{-H}^+)\text{-C}(\text{+H}^+)_{\text{PT}}$ is considered as the proton-transferred product of the $\text{H}^+\text{G}_{\text{N}7}\text{-C}$ structure. The transferred proton is colored black and the added proton colored gray. Three possible hydrogen-bonded proton-transfer pathways (1), (2), and (3) are shown in Scheme 1. We consider three paths for each protonated cation isomer and analyze the probabilities of every proton-transfer pathway theoretically. The optimized gas phase geometries of these protonated cations are reported in Figures 1–12, in which the bond distances for each trio of structures are given in angstroms. In addition, side views of the cations which lose the planarity of the GC base pair are shown. All the natures of the stationary points were checked via vibrational frequency computations. The structural changes and energy differences among the conventional protonated guanine-cytosine, the associated transition

states, and the hydrogen-bonded proton-transferred products are discussed in this paper.

3.1. Geometries and Relative Energies. The relative energies of the $(\text{GC+H})^+$ and $(\text{GC+H})^+_{\text{PT}}$ structures, evaluated with respect to the lowest-energy structure, $\text{H}^+\text{G}_{\text{N}7}\text{-C}$ with the proton attached at the guanine N_7 position, are presented in Table 1. ΔE expresses the energy difference between the proton-transferred product and the conventional protonated GC base pair without the ZPVE corrections. In comparison with the anionic $(\text{GC+H})^-$ radical structure,⁵⁴ the cation species $(\text{GC+H})^+$ undergoes less dramatic geometry perturbations with respect to the proton transfer. Sites N_7 , O_6 , and N_3 in guanine and N_3 in cytosine have the largest proton affinities,¹⁸ and the corresponding protonated base pairs have the lowest relative energies. We now consider the different proton-transfer possibilities in a systematic manner.

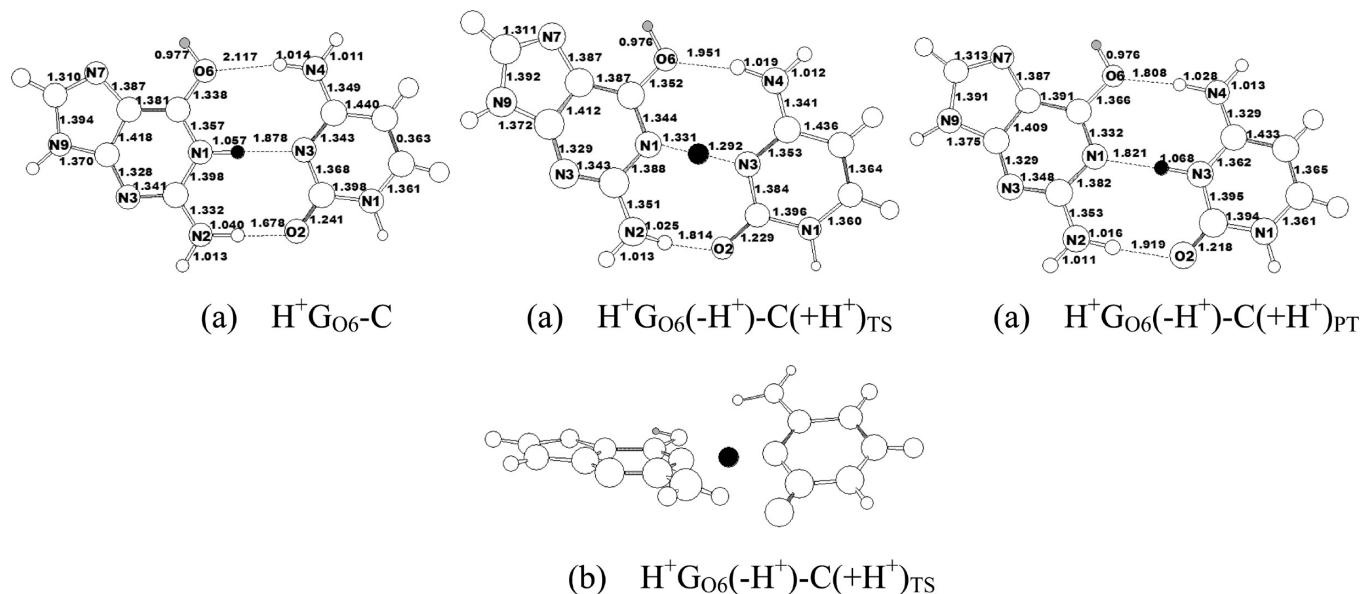


Figure 5. (a) The optimized conventional protonated structure $\text{H}^+\text{G}_{\text{O}6}\text{-C}$, transition state (TS) structure $\text{H}^+\text{G}_{\text{O}6}(\text{-H}^+)\text{-C}(\text{+H}^+)\text{TS}$, and proton-transferred product (PT) $\text{H}^+\text{G}_{\text{O}6}(\text{-H}^+)\text{-C}(\text{+H}^+)\text{PT}$. (b) A side view of the structure $\text{H}^+\text{G}_{\text{O}6}(\text{-H}^+)\text{-C}(\text{+H}^+)\text{TS}$.

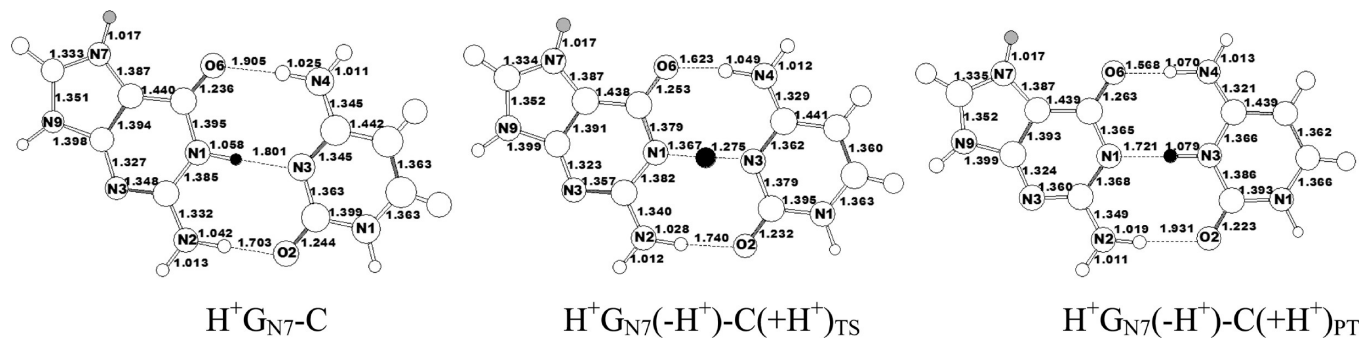


Figure 6. The optimized conventional protonated structure $\text{H}^+\text{G}_{\text{N}7}\text{-C}$, transition state (TS) structure $\text{H}^+\text{G}_{\text{N}7}(\text{-H}^+)\text{-C}(\text{+H}^+)\text{TS}$, and proton-transferred product (PT) $\text{H}^+\text{G}_{\text{N}7}(\text{-H}^+)\text{-C}(\text{+H}^+)\text{PT}$.

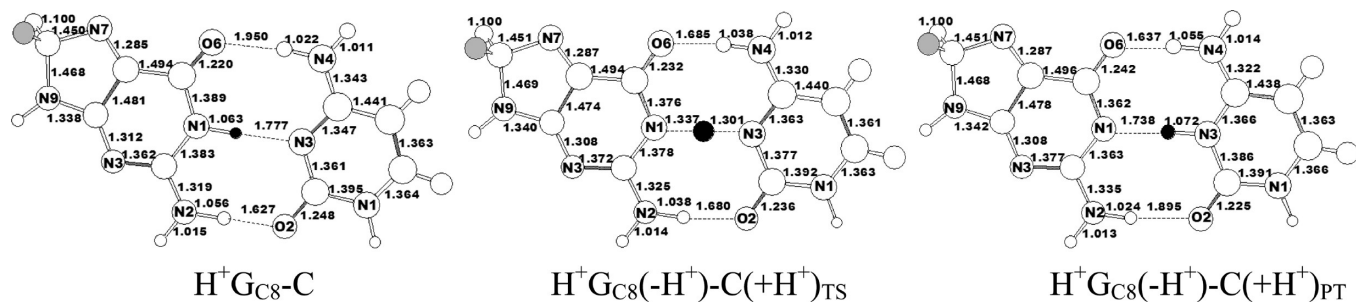


Figure 7. The optimized conventional protonated structure $\text{H}^+\text{G}_{\text{C}8}\text{-C}$, transition state (TS) structure $\text{H}^+\text{G}_{\text{C}8}(\text{-H}^+)\text{-C}(\text{+H}^+)\text{TS}$, and proton-transferred product (PT) $\text{H}^+\text{G}_{\text{C}8}(\text{-H}^+)\text{-C}(\text{+H}^+)\text{PT}$.

If the proton attaches to the C_2 site of guanine, abbreviated by the structure $\text{H}^+\text{G}_{\text{C}2}\text{-C}$, the H_1 proton of guanine is shifted to the N_3 site of cytosine following the proton-transfer pathway 1 (Figure 1). As a result, some important electronic changes take place in the vicinity of the transferred H_1 . With the H_1 loss from guanine, the bond lengths $\text{N}_1\text{-C}_2(\text{G})$ and $\text{N}_1\text{-C}_6(\text{G})$

are shortened by 0.023 and 0.018 Å, respectively, which result in $\text{C}_2\text{-N}_3(\text{G})$ and $\text{C}_6\text{-O}_6(\text{G})$ bond elongation. When atom N_3 of the cytosine combine the shifted H_1 , the $\text{N}_3=\text{C}_4(\text{C})$ π bond is broken and the $\text{C}_2\text{-N}_3(\text{C})$ and $\text{N}_3\text{-C}_4(\text{C})$ bonds there upon increase by 0.024 and 0.022 Å, while the $\text{C}_2\text{-O}_2(\text{C})$ and $\text{C}_4\text{-N}_4(\text{C})$ decrease by 0.021 and 0.024 Å, respectively. The

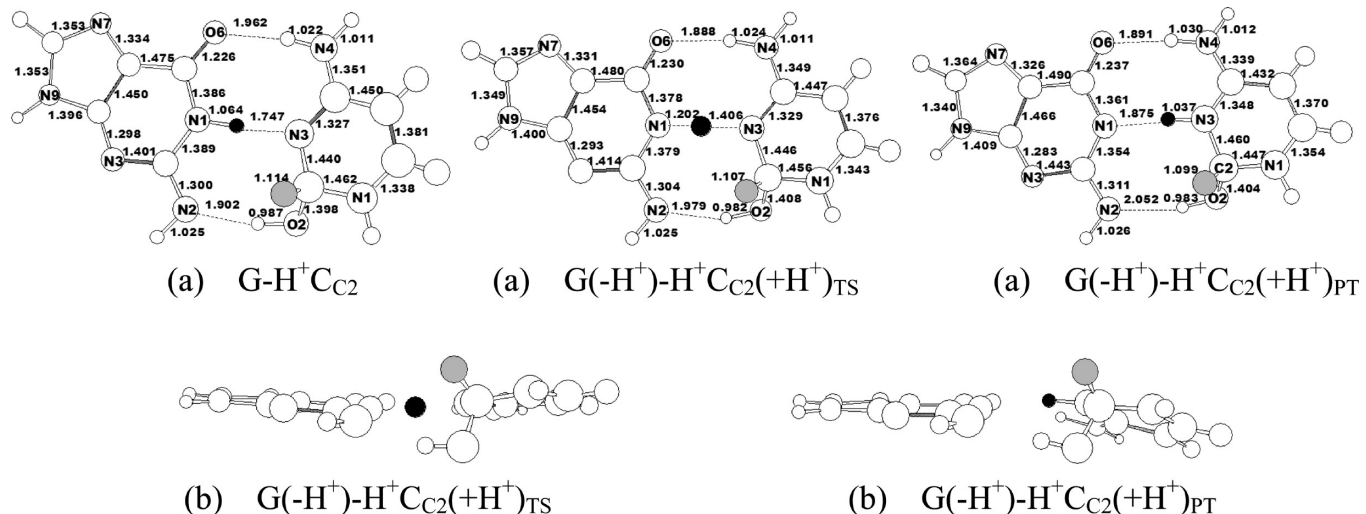


Figure 8. (a) The optimized conventional protonated structure $\text{G}-\text{H}^+\text{C}_{\text{C}2}$, transition state (TS) structure $\text{G}(-\text{H}^+)-\text{H}^+\text{C}_{\text{C}2}(+\text{H}^+)\text{TS}$, and proton-transferred product (PT) $\text{G}(-\text{H}^+)-\text{H}^+\text{C}_{\text{C}2}(+\text{H}^+)\text{PT}$. (b) Side views of the structures $\text{G}(-\text{H}^+)-\text{H}^+\text{C}_{\text{C}2}(+\text{H}^+)\text{TS}$ and $\text{G}(-\text{H}^+)-\text{H}^+\text{C}_{\text{C}2}(+\text{H}^+)\text{PT}$.

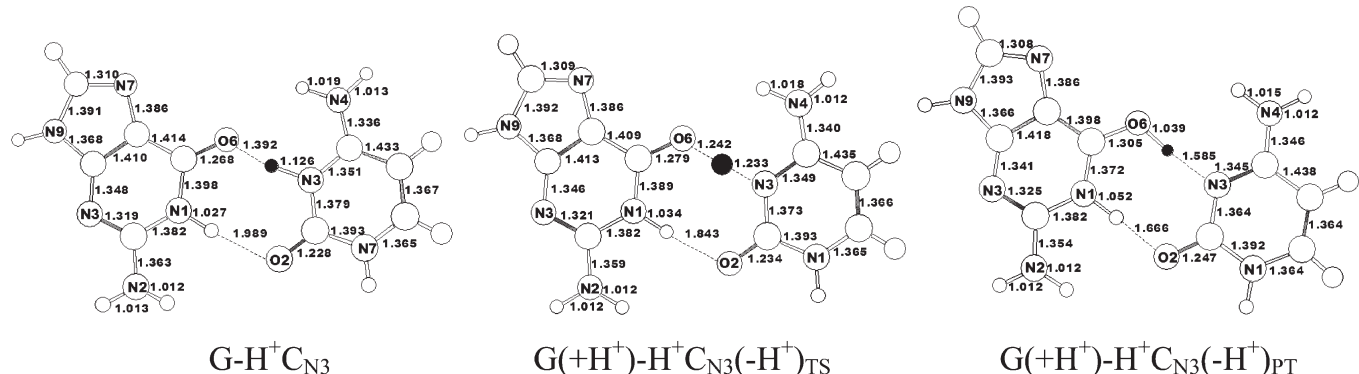


Figure 9. The optimized conventional protonated structure $\text{G}-\text{H}^+\text{C}_{\text{N}3}$, transition state (TS) structure $\text{G}(+\text{H}^+)-\text{H}^+\text{C}_{\text{N}3}(-\text{H}^+)\text{TS}$, and proton-transferred product (PT) $\text{G}(+\text{H}^+)-\text{H}^+\text{C}_{\text{N}3}(-\text{H}^+)\text{PT}$.

energy of the structure $\text{H}^+\text{G}_{\text{C}2}\text{-C}$ lies 77.2 kcal/mol (without ZPVE correction) above the lowest-energy cation, structure $\text{H}^+\text{G}_{\text{N}7}\text{-C}$. The corresponding proton-transferred product $\text{H}^+\text{G}_{\text{C}2}\text{(-H}^+)\text{-C(+H}^+)\text{PT}$, retaining the C_1 symmetry of the $\text{H}^+\text{G}_{\text{C}2}\text{-C}$ structure, lies 76.2 kcal/mol (Table 1) above the lowest-energy $\text{H}^+\text{G}_{\text{N}7}\text{-C}$.

The structure $\text{H}^+\text{G}_{\text{N}3}\text{-C}$ (Figure 2), resulting from proton addition to the N_3 site of guanine, keeps the guanine and cytosine in the same plane (C_s symmetry) during the process of proton transfer. The proton-transferred product $\text{H}^+\text{G}_{\text{N}3}\text{(-H}^+)\text{-C(+H}^+)\text{PT}$ lies 9.0 kcal/mol higher than the lowest-energy structure $\text{H}^+\text{G}_{\text{N}7}\text{-C}$ and 0.6 kcal/mol higher than the conventional protonated $\text{H}^+\text{G}_{\text{N}3}\text{-C}$. The proton-transferred product $\text{H}^+\text{G}_{\text{C}4}\text{(-H}^+)\text{-C(+H}^+)\text{PT}$ is formed as the H_1 proton of the N_1 site of G transfers to the N_3 site of C. The latter structure is predicted to lie 2.6 kcal/mol higher than the corresponding structure $\text{H}^+\text{G}_{\text{C}4}\text{-C}$ (Figure 3). In Figures 2 and 3, the proton transfer follows pathway 1, i.e., H_1 transfers from the N_1 site of the purine to the N_3 site of the pyrimidine, which necessarily results in strengthening of the $\text{N}_1-\text{C}_2\text{-G}$ and $\text{N}_1-\text{C}_6\text{(G)}$ bonds and weakening of the $\text{N}_3-\text{C}_2\text{(C)}$ and $\text{N}_3-\text{C}_4\text{(C)}$ bonds. Simultaneously, the bond lengths $\text{C}_2-\text{N}_2\text{(G)}$ and $\text{C}_6-\text{O}_6\text{(G)}$ increase, but the distances $\text{C}_2-\text{O}_2\text{(C)}$ and $\text{C}_4-\text{N}_4\text{(C)}$ decrease.

Structure $\text{H}^+\text{G}_{\text{C}5}\text{-C}$ and structure $\text{H}^+\text{G}_{\text{C}6}\text{-C}$, shown in Figure 4, are found by proton addition to the C_5 or C_6 sites of guanine. It is interesting that when a proton attaches to the C_6 site of guanine, the structure collapses to the proton-transferred product $\text{H}^+\text{G}_{\text{C}5}\text{(-H}^+)\text{-C(+H}^+)\text{PT}$, following the proton-transfer pathway 1, in which the H_1 proton of guanine transfers to the N_3 site of cytosine. The energies of the reactant and product for the proton-transfer reaction are predicted to lie 21.5 and 20.3 kcal/mol higher than the global minimum, respectively.

The structure $\text{H}^+\text{G}_{\text{O}6}\text{-C}$ (Figure 5a) is formed when a proton adds to the guanine O_6 site. The guanine ring and the cytosine ring twist during the process of proton-transfer reaction, as shown in Figure 5b. The transition state $\text{H}^+\text{G}_{\text{O}6}\text{(-H}^+)\text{-C(+H}^+)\text{TS}$ in C_1 symmetry presents a propellerlike twist. The interplanar angle between the two bases is -146.1° (dihedral angle $\text{G}_{\text{C}2}\text{-G}_{\text{N}1}\text{-C}_{\text{N}3}\text{-C}_{\text{C}4}$). However, the product structure $\text{H}^+\text{G}_{\text{O}6}\text{(-H}^+)\text{-C(+H}^+)\text{PT}$ returns to planarity and maintains the original C_s symmetry of the structure $\text{H}^+\text{G}_{\text{O}6}\text{-C}$. The eight adjacent bonds to the transferred H_1 proton change greatly compared with the structure $\text{H}^+\text{G}_{\text{O}6}\text{-C}$. The $\text{N}_1-\text{C}_6\text{(G)}$, $\text{N}_1-\text{C}_2\text{(G)}$, $\text{N}_4-\text{C}_4\text{(C)}$, and $\text{C}_2-\text{O}_2\text{(C)}$ bonds are shortened, while the $\text{C}_6-\text{O}_6\text{(G)}$, $\text{C}_2-\text{N}_2\text{(G)}$, $\text{N}_3-\text{C}_4\text{(C)}$, and $\text{N}_3-\text{C}_2\text{(C)}$ bonds are significantly elongated. The total energy of the

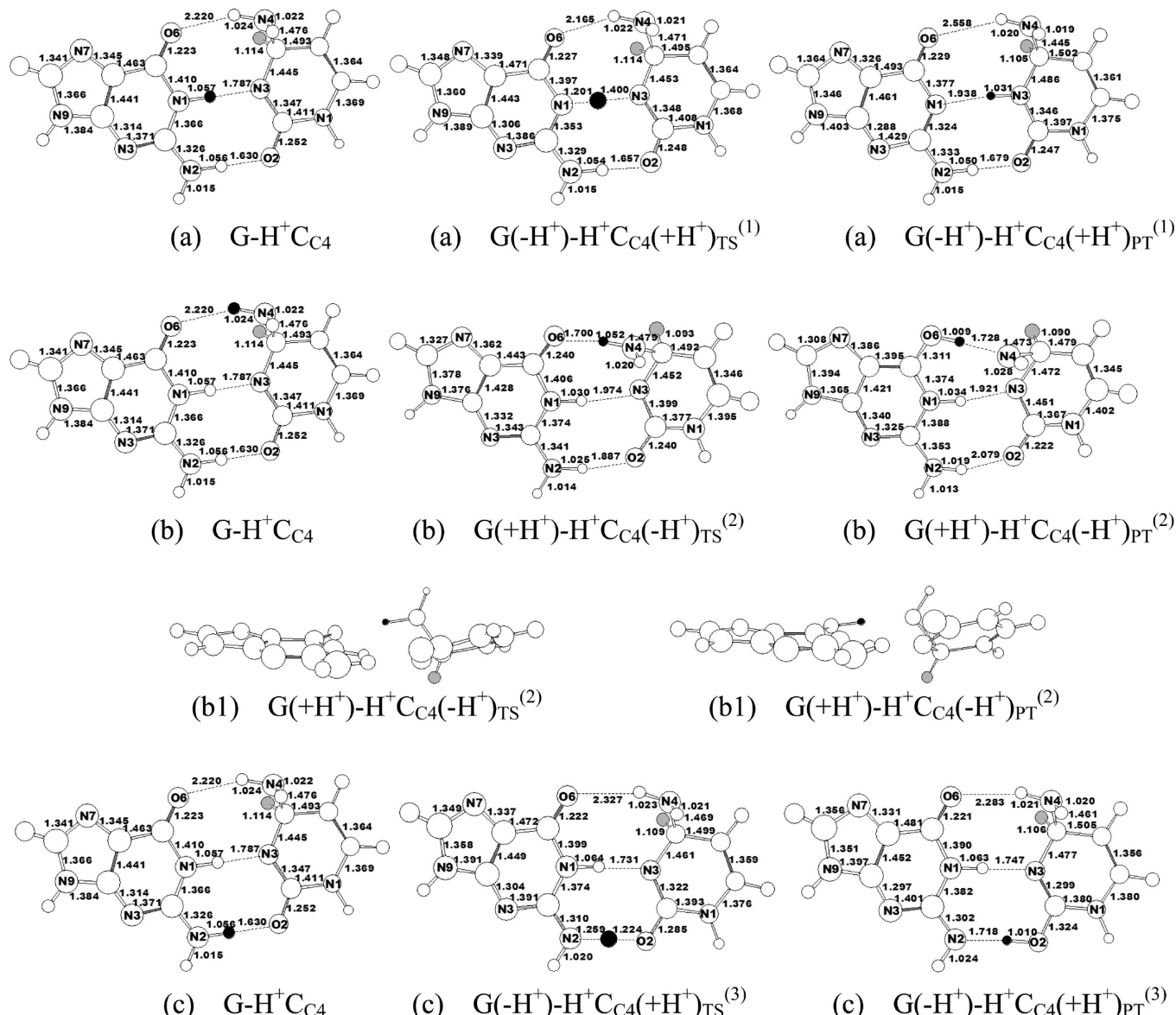


Figure 10. (a–c) The optimized conventional protonated structure $\text{G}-\text{H}^+\text{C}_{\text{C}4}$, transition state (TS) structure $\text{G}(-\text{H}^+)-\text{H}^+\text{C}_{\text{C}4}(+\text{H}^+)\text{TS}$, and proton-transferred product (PT) $\text{G}(-\text{H}^+)-\text{H}^+\text{C}_{\text{C}4}(+\text{H}^+)\text{PT}$. The label (b1) designates side views of the structures $\text{G}(\text{H}^+)-\text{H}^+\text{C}_{\text{C}4}(-\text{H}^+)\text{TS}^{(2)}$ and $\text{G}(\text{H}^+)-\text{H}^+\text{C}_{\text{C}4}(-\text{H}^+)\text{PT}^{(2)}$.

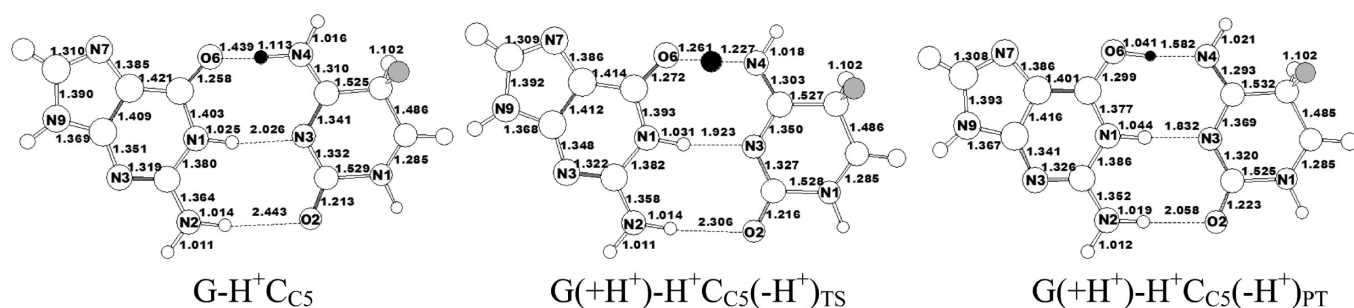


Figure 11. The optimized conventional protonated structure $\text{G}-\text{H}^+\text{C}_{\text{C}5}$, transition state (TS) structure $\text{G}(\text{H}^+)-\text{H}^+\text{C}_{\text{C}5}(-\text{H}^+)\text{TS}$, and proton-transferred product (PT) $\text{G}(\text{H}^+)-\text{H}^+\text{C}_{\text{C}5}(-\text{H}^+)\text{PT}$.

structure $\text{H}^+\text{G}_{\text{O}6}\text{-C}$ is predicted to be 6.8 kcal/mol higher than the lowest-energy structure $\text{H}^+\text{G}_{\text{N}7}\text{-C}$, and the structure

$\text{H}^+\text{G}_{\text{O}6}(-\text{H}^+)-\text{C}(+\text{H}^+)\text{PT}$ is predicted to lie 8.9 kcal/mol higher than structure $\text{H}^+\text{G}_{\text{N}7}\text{-C}$.

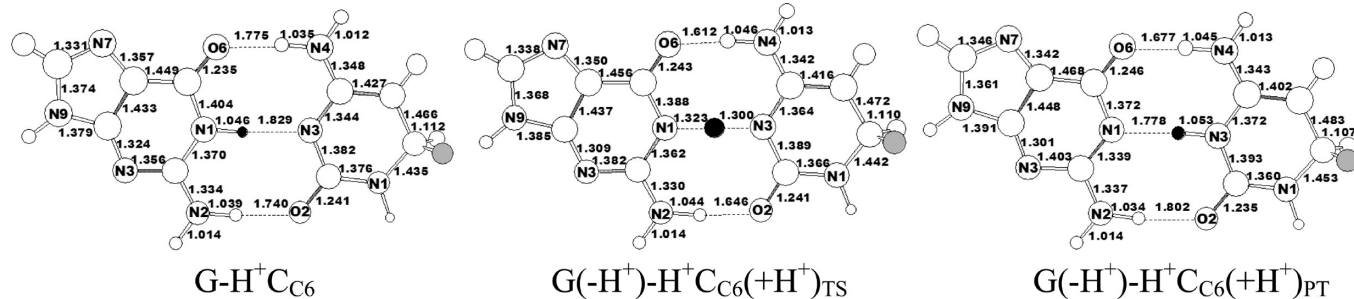


Figure 12. The optimized conventional protonated structure $\text{G}-\text{H}^+\text{C}_{\text{C}6}$, transition state (TS) structure $\text{G}(-\text{H}^+)-\text{H}^+\text{C}_{\text{C}6}(\text{H}^+)\text{TS}$, and proton-transferred product (PT) $\text{G}(-\text{H}^+)-\text{H}^+\text{C}_{\text{C}6}(\text{H}^+)\text{PT}$.

Table 1. Classical and Corrected (Zero-Point Vibrational Energy) Relative Energies (kcal/mol) and Energy Differences ΔE (kcal/mol) between the Conventional Protonated ($\text{GC}+\text{H}$)⁺ and Proton-Transferred Product ($\text{GC}+\text{H}$)⁺_{PT} (See Scheme 1 for the Atom Numbering)

conventional protonated ($\text{GC}+\text{H}$) ⁺			proton-transferred product ($\text{GC}+\text{H}$) ⁺ _{PT}			
($\text{GC}+\text{H}$) ⁺	relative energies	relative energies (ZPVE corrected)	($\text{GC}+\text{H}$) ⁺ _{PT}	relative energies	relative energies (ZPVE corrected)	ΔE
$\text{H}^+\text{G}_{\text{N}7}\text{-C}$	0.0	0.0	$\text{H}^+\text{G}_{\text{N}7}(-\text{H}^+)-\text{C}(\text{H}^+)\text{PT}$	4.0	3.5	4.0
$\text{G}-\text{H}^+\text{C}_{\text{N}3}$	3.0	1.5	$\text{G}(\text{H}^+)-\text{H}^+\text{C}_{\text{N}3}(-\text{H}^+)\text{PT}$	1.9	0.8	-1.1
$\text{H}^+\text{G}_{\text{O}6}\text{-C}$	6.8	6.3	$\text{H}^+\text{G}_{\text{O}6}(-\text{H}^+)-\text{C}(\text{H}^+)\text{PT}$	8.9	8.6	2.1
$\text{H}^+\text{G}_{\text{N}3}\text{-C}$	8.4	7.4	$\text{H}^+\text{G}_{\text{N}3}(-\text{H}^+)-\text{C}(\text{H}^+)\text{PT}$	9.0	7.8	0.6
$\text{H}^+\text{G}_{\text{C}8}\text{-C}$	17.8	16.7	$\text{H}^+\text{G}_{\text{C}8}(-\text{H}^+)-\text{C}(\text{H}^+)\text{PT}$	19.5	18.4	1.7
$\text{H}^+\text{G}_{\text{C}5}\text{-C}$	20.3	19.0	$\text{H}^+\text{G}_{\text{C}5}(-\text{H}^+)-\text{C}(\text{H}^+)\text{PT}$	21.5	20.3	1.2
$\text{H}^+\text{G}_{\text{C}6}\text{-C}$	21.5	20.3	$\text{H}^+\text{G}_{\text{C}6}(-\text{H}^+)-\text{C}(\text{H}^+)\text{PT}$	20.3	19.0	-1.2
$\text{G}-\text{H}^+\text{C}_{\text{O}2}$	26.8	25.5	Collapses to $\text{G}-\text{H}^+\text{C}_{\text{O}2}$			
$\text{G}-\text{H}^+\text{C}_{\text{C}5}$	44.9	41.9	$\text{G}(\text{H}^+)-\text{H}^+\text{C}_{\text{C}5}(-\text{H}^+)\text{PT}$	43.6	41.3	-1.3
$\text{H}^+\text{G}_{\text{C}4}\text{-C}$	53.8	51.8	$\text{H}^+\text{G}_{\text{C}4}(-\text{H}^+)-\text{C}(\text{H}^+)\text{PT}$	56.4	54.1	2.6
$\text{G}-\text{H}^+\text{C}_{\text{C}6}$	76.7	73.4	$\text{G}(-\text{H}^+)-\text{H}^+\text{C}_{\text{C}6}(\text{H}^+)\text{PT}$	78.6	75.5	1.9
$\text{H}^+\text{G}_{\text{C}2}\text{-C}$	77.2	74.4	$\text{H}^+\text{G}_{\text{C}2}(-\text{H}^+)-\text{C}(\text{H}^+)\text{PT}$	76.2	73.4	-1.0
$\text{G}-\text{H}^+\text{C}_{\text{C}2}$	104.9	101.6	$\text{G}(-\text{H}^+)-\text{H}^+\text{C}_{\text{C}2}(\text{H}^+)\text{PT}$	95.5	93.4	-9.4
$\text{G}-\text{H}^+\text{C}_{\text{C}4}$	109.9	106.0	$\text{G}(-\text{H}^+)-\text{H}^+\text{C}_{\text{C}4}(\text{H}^+)\text{PT}^{(1)}$ $\text{G}(\text{H}^+)-\text{H}^+\text{C}_{\text{C}4}(-\text{H}^+)\text{PT}^{(2)}$ $\text{G}(-\text{H}^+)-\text{H}^+\text{C}_{\text{C}4}(\text{H}^+)\text{PT}^{(3)}$	99.1 82.3 109.3	96.2 81.1 105.9	-10.8 -27.6 -0.6

The structure $\text{H}^+\text{G}_{\text{N}7}\text{-C}$ with the proton attached at the guanine N_7 position is shown in Figure 6, which is the lowest-energy protonated GC structure in this work. The surrounding bonds of the proton-transfer site display significant changes after the H_1 proton of guanine transfers to the N_3 site of cytosine. The $\text{C}_6\text{-O}_6$ and $\text{C}_2\text{-N}_3$ bonds in the guanine moiety and the $\text{C}_4\text{-N}_3$ and $\text{C}_2\text{-N}_3$ bonds in the cytosine moiety are elongated. The $\text{C}_6\text{-N}_1$ and $\text{C}_2\text{-N}_1$ bonds in guanine and the $\text{C}_4\text{-N}_4$ and $\text{C}_2\text{-O}_2$ bonds in cytosine are significantly shortened. The corresponding proton-transferred product structure $\text{H}^+\text{G}_{\text{N}7}(-\text{H}^+)-\text{C}(\text{H}^+)\text{PT}$ is predicted to lie 4.0 kcal/mol above structure $\text{H}^+\text{G}_{\text{N}7}\text{-C}$.

The cation $\text{H}^+\text{G}_{\text{C}8}(-\text{H}^+)-\text{C}(\text{H}^+)\text{PT}$ (Figure 7) is the proton-transferred product of structure $\text{H}^+\text{G}_{\text{C}8}\text{-C}$, resulting from a proton adding to the C_8 site of guanine, and lies 19.5 kcal/mol higher than the global minimum structure $\text{H}^+\text{G}_{\text{N}7}\text{-C}$. Because the C_8 site is far away from the hydrogen bond, the bond lengths perturbations are slight with proton attachment and proton transfer.

The products of the proton-transferred ($\text{GC}+\text{H}$)⁺ isomers have been identified theoretically, except for the structure $\text{G}-\text{H}^+\text{C}_{\text{O}2}$.

When a proton is added to the oxygen atom of the cytosine, the hydrogen bond distances become longer than 3.3 Å.¹⁸ That is, no proton transfer is found. The isomer $\text{G}-\text{H}^+\text{C}_{\text{C}2}$ (Figure 8a) is produced when a proton is added to position C_2 of cytosine. This protonated structure undergoes dramatic geometry perturbations during the proton-transfer reaction. When a proton adds to the C_2 site of cytosine, atom O_2 of cytosine abstracts a hydrogen atom of the amino group from guanine to form the conventional protonated cation $\text{G}-\text{H}^+\text{C}_{\text{C}2}$.¹⁸ The proton-transferred product $\text{G}(-\text{H}^+)-\text{H}^+\text{C}_{\text{C}2}(\text{H}^+)\text{PT}$ is formed by guanine's H_1 proton transfer to the N_3 site of cytosine. During the proton-transfer reaction, the planarity of the GC rings is destroyed; the dihedral angle of guanine and cytosine is 146.3° (dihedral angle $\text{G}_{\text{C}2}\text{-G}_{\text{N}1}\text{-C}_{\text{N}3}\text{-C}_{\text{C}4}$). The bond distances $\text{C}_2\text{-N}_3$ and $\text{C}_4\text{-C}_5$ of guanine are increased by 0.042 and 0.016 Å, respectively, and the $\text{C}_4\text{-C}_5$ bond length of cytosine is decreased 0.018 Å in the proton-transferred product, compared to the conventional protonated structure. However, since $\text{G}(-\text{H}^+)-\text{H}^+\text{C}_{\text{C}2}(\text{H}^+)\text{PT}$ lies much higher (95.5 kcal/mol) than the lowest-energy cation $\text{H}^+\text{G}_{\text{N}7}\text{-C}$, the probability that this dramatic GC structural

Table 2. NBO Charge Distribution for the Guanine and Cytosine Moieties in the Conventional Protonated ($(GC+H)^+$) and Proton-Transferred Product ($(GC+H)^+_{PT}$)

structure	NBO charge			
	G moiety	C moiety	G_{PT} moiety	C_{PT} moiety
$H^+G_{C2}-C$	0.89	0.11	0.16	0.84
$H^+G_{N3}-C$	0.85	0.15	0.16	0.84
$H^+G_{C4}-C$	0.88	0.12	0.16	0.84
$H^+G_{C5}-C$	0.85	0.15	0.15	0.85
$H^+G_{O6}-C$	0.88	0.12	0.10	0.90
$H^+G_{N7}-C$	0.89	0.11	0.18	0.82
$H^+G_{C8}-C$	0.86	0.14	0.15	0.85
$G-H^+C_{C2}$	0.42	0.58	0.12	0.88
$G-H^+C_{N3}$	0.15	0.85	0.80	0.20
$G-H^+C_{C4}^{(1)}$	0.67	0.33	0.58	0.42
$G-H^+C_{C5}$	0.11	0.89	0.79	0.21
$G-H^+C_{C6}$	0.67	0.33	0.20	0.80

deformation causes a significant DNA lesion is small. The total energy of the conventional protonated isomer $G-H^+C_{C2}$ is 9.4 kcal/mol higher than the corresponding proton-transferred product structure $G(-H^+)-H^+C_{C2}(+H^+)_{PT}$.

Structure $G(+H^+)-H^+C_{N3}(-H^+)_{PT}$ (Figure 9) is the proton-transfer product from proton addition to atom N_3 of cytosine and lies only 1.9 kcal/mol above the global minimum structure $H^+G_{N7}-C$. The corresponding conventional protonated structure $G-H^+C_{N3}$ has an energy 1.1 kcal/mol higher than that of $G(+H^+)-H^+C_{N3}(-H^+)_{PT}$. During the proton-transfer process, the additional H_3 proton of cytosine transfers to guanine O_6 , which causes the adjoined $C_6-N_1(G)$ and $C_6-C_5(G)$ bond distances to decrease by 0.026 and 0.016 Å, respectively, while the $C_6-O_6(G)$ distance increases by 0.037 Å.

When a proton attaches to the C_4 site of the cytosine, structure $G-H^+C_{C4}$ (Figure 10) is formed. For the structure $G-H^+C_{C4}$, the highest energy was found, lying 109.9 kcal/mol above the global minimum structure $H^+G_{N7}-C$. Three possible hydrogen-bonded proton-transfer pathways (1), (2), and (3) are found here. The proton-transferred product $G(-H^+)-H^+C_{C4}(+H^+)_{PT}^{(1)}$ from the first proton-transfer pathway and $G(+H^+)-H^+C_{C4}(-H^+)_{PT}^{(2)}$ from the second proton-transfer pathway lie 10.8 and 27.6 kcal/mol lower in energy than structure $G-H^+C_{C4}$, respectively. The product structure $G(+H^+)-H^+C_{C4}(-H^+)_{PT}^{(2)}$ loses planarity, with the dihedral angle 73.8° (dihedral angle $G_{C2}-G_{N1}-C_{N3}-C_{C6}$) between guanine and cytosine (part b1 of Figure 10). The proton-transferred product $G(-H^+)-H^+C_{C4}(+H^+)_{PT}^{(3)}$ resulting from the third proton-transfer pathway has nearly the same energy as the corresponding conventional protonated structure. However, the energies of the transition state structures $G(+H^+)-H^+C_{C4}(-H^+)_{TS}^{(2)}$ and $G(-H^+)-H^+C_{C4}(+H^+)_{TS}^{(3)}$ are higher than that of the transition state structure $G(-H^+)-H^+C_{C4}(+H^+)_{TS}^{(1)}$. Thus in the following section we discuss only the proton-transferred product $G(-H^+)-H^+C_{C4}(+H^+)_{PT}^{(1)}$ from the first proton-transfer pathway with the lowest proton-transfer energy barrier.

Structure $G-H^+C_{C5}$, shown in Figure 11, is the cation formed by adding a proton to the C_5 site of cytosine. The cytosine H_{4a} proton transfers to the guanine O_6 site in the structure $G-H^+C_{C5}$. Such a selection of proton-transfer path is related to the electric charge redistribution and hydrogen bond length change during

Table 3. Hydrogen Bond Lengths for the $(GC+H)^+$, $(GC+H)^+_{TS}$, and $(GC+H)^+_{PT}$ Base Pair Cations

species	hydrogen bonds	bond lengths (Å)		
		$(GC+H)^+$	$(GC+H)^+_{TS}$	$(GC+H)^+_{PT}$
$H^+G_{C2}-C$	$O \cdots H-N$	2.983	2.769	2.662
	$N-H \cdots N$	2.786	2.603	2.861
	$N-H \cdots O$	2.915	2.989	3.124
	$H^+G_{N3}-C$	$O \cdots H-N$	2.893	2.675
		$N-H \cdots N$	2.829	2.638
	$H^+G_{C4}-C$	$N-H \cdots O$	2.650	2.687
		$O \cdots H-N$	3.000	2.747
		$N-H \cdots N$	2.846	2.624
$H^+G_{C5}-C$	$N-H \cdots O$	2.748	2.789	2.969
	$H^+G_{O6}-C$	$O \cdots H-N$	2.994	2.757
		$N-H \cdots N$	2.822	2.622
	$H^+G_{N7}-C$	$N-H \cdots O$	2.685	2.740
		$O \cdots H-N$	3.131	2.970
		$N-H \cdots N$	2.935	2.623
	$H^+G_{C8}-C$	$N-H \cdots O$	2.718	2.839
		$O \cdots H-N$	2.930	2.672
		$N-H \cdots N$	2.859	2.642
$G-H^+C_{C2}$	$N-H \cdots O$	2.745	2.768	2.950
	$G-H^+C_{N3}$	$O \cdots H-N$	2.972	2.723
		$N-H \cdots N$	2.840	2.638
		$N-H \cdots O$	2.683	2.718
	$G-H^+C_{C4}$	$O \cdots H-N$	2.984	2.912
		$N-H \cdots N$	2.811	2.608
		$N \cdots H-O$	2.889	2.961
$G-H^+C_{C5}$	$O \cdots H-N$	2.518	2.475	2.624
	$G-H^+C_{C6}$	$N-H \cdots O$	3.016	2.877
		$O \cdots H-N$	3.244	3.187
		$N-H \cdots N$	2.844	2.601
	$G-H^+C_{N7}$	$N-H \cdots O$	2.686	2.711
		$O \cdots H-N$	2.552	2.488
		$N-H \cdots N$	3.051	2.954
$G-H^+C_{C6}$	$N-H \cdots O$	3.457	3.320	3.077
	$G-H^+C_{C2}$	$O \cdots H-N$	2.810	2.658
		$N-H \cdots N$	2.875	2.623
		$N-H \cdots O$	2.779	2.690

the proton transfer. The corresponding structure $G(+H^+)-H^+C_{C5}(-H^+)_{PT}$ lies 43.6 kcal/mol higher than structure $H^+G_{N7}-C$. The transfer of the H_{4a} proton mainly brings about the elongation of the $C_6-O_6(G)$ and $C_4-N_3(C)$ bonds. Meanwhile, the bond distances $C_6-N_1(G)$, $C_6-N_5(G)$, and $C_4-N_4(C)$ are decreased.

For structure $G-H^+C_{C6}$ (Figure 12), the proton-transfer pathway is analogous to structure $G-H^+C_{C4}$, as the guanine H_1 proton still transfers in the reaction. The transition state structure $G(-H^+)-H^+C_{C6}(+H^+)_{TS}$ and proton-transferred structure $G(-H^+)-H^+C_{C6}(+H^+)_{PT}$ are of C_s symmetry, which differs from the conventional protonated structure $G-H^+C_{C6}$ with C_1 symmetry. The structure $G(-H^+)-H^+C_{C6}(+H^+)_{PT}$ lies 1.9 kcal/mol higher than structure $G-H^+C_{C6}$.

3.2. NBO Charge Distributions and Hydrogen Bonds. The NBO charges and the hydrogen bond lengths are presented in

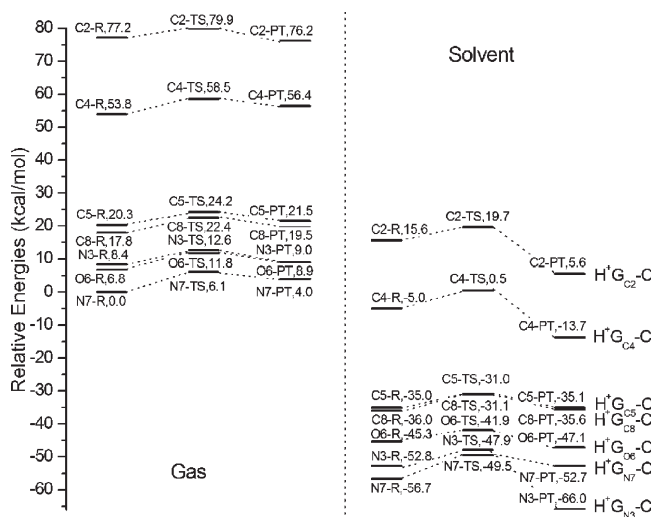


Figure 13. Energy profiles for single proton transfer in which the proton is attached to the guanine moiety. The results on the left refer in the gas phase. Those on the right refer to water solvent obtained from PCM. The energies are given with respect to the conventional protonated structure $\text{H}^+\text{G}_{\text{N}7}\text{-C}$ ($\text{N}7\text{-R}$) in the gas phase.

Table 2 and Table 3. Usually, the pathway for proton transfer depends on the acidity of the base moiety and the hydrogen bond length. For most conventional protonated structures, the positive charge is mainly located at the guanine moiety and redistributed primarily on cytosine after proton transfer. This redistribution does not happen when the proton is added to the C_2 , N_3 , and C_5 sites of cytosine (Table 2). Comparing the hydrogen bond lengths for the conventional protonated structures $(\text{GC}+\text{H})^+$, transition state structures $(\text{GC}+\text{H})^+_{\text{TS}}$, and products of the proton-transferred $(\text{GC}+\text{H})^+_{\text{PT}}$ base pair cations (Table 3), the hydrogen bonds $(\text{G})\text{O}_6 \cdots \text{H}-\text{N}_4(\text{C})$ of $(\text{GC}+\text{H})^+_{\text{PT}}$ are shortened except $\text{G}-\text{H}^+\text{C}_{\text{C}4}^{(1)}$ and $\text{G}-\text{H}^+\text{C}_{\text{C}5}$. The hydrogen bonds $(\text{G})\text{N}_1-\text{H} \cdots \text{N}_3(\text{C})$ of $(\text{GC}+\text{H})^+_{\text{TS}}$ are shortened, and the hydrogen bonds $(\text{G})\text{N}_2-\text{H} \cdots \text{O}_2(\text{C})$ of $(\text{GC}+\text{H})^+_{\text{PT}}$ are lengthened except in $\text{G}-\text{H}^+\text{C}_{\text{C}5}$. For $\text{G}-\text{H}^+\text{C}_{\text{N}3}$, there are only two hydrogen bonds $(\text{G})\text{O}_6 \cdots \text{H}-\text{N}_3(\text{C})$ and $(\text{G})\text{N}_1-\text{H} \cdots \text{O}_2(\text{C})$ between the guanine and cytosine base moieties.

When a proton attaches to the guanine moiety, the proton transfer follows the hydrogen bond $(\text{G})\text{N}_1-\text{H} \cdots \text{N}_3(\text{C})$, i.e., the H_1 proton of the guanine moiety transfers to N_3 of cytosine. Three factors contributed to this proton-transfer pathway. First, the acidity of the guanine is necessarily stronger than that for cytosine. For the conventional protonated structures, the positive charge is mainly located at the protonated guanine moiety, whose NBO charges are in the range of 0.85–0.89, whereas the corresponding cytosine moiety has NBO charges of only 0.11–0.15 (Table 2). The proton prefers to transfer from guanine with its high NBO charge to cytosine with the low NBO charge. Second, the hydrogen bonds $(\text{G})\text{N}_1-\text{H} \cdots \text{N}_3(\text{C})$ and $(\text{G})\text{N}_2-\text{H} \cdots \text{O}_2(\text{C})$ are shorter than hydrogen bond $(\text{G})\text{O}_6 \cdots \text{H}-\text{N}_4(\text{C})$, which is also conducive to the proton transfer from guanine to cytosine. As a third factor, site N_3 in cytosine has the largest proton affinity (244.0 kcal/mol) among the three accepted proton positions; the other two sites O_6 in guanine and O_2 in cytosine possessing 240.3 and 220.2 kcal/mol, respectively.¹⁸ Thus, when the proton is attached to

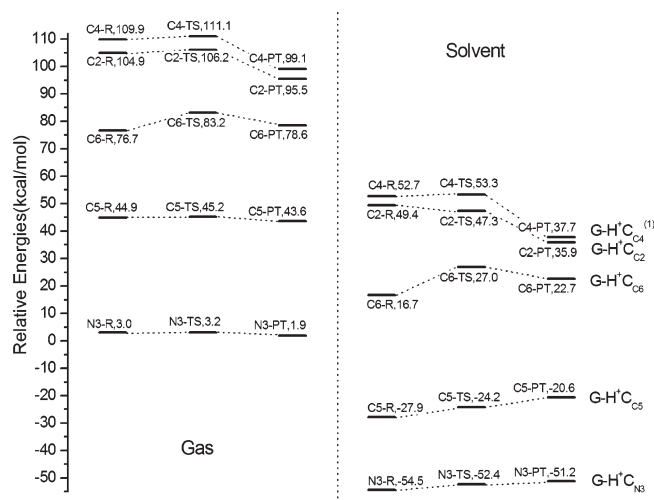


Figure 14. Energy profiles for single proton transfer in which the proton is attached to the cytosine moiety. The results on the left are for the gas phase, while those on the right refer to PCM water solvent. The energies are given with respect to the conventional protonated structure $\text{H}^+\text{G}_{\text{N}7}\text{-C}$ ($\text{N}7\text{-R}$) in the gas phase.

the guanine moiety of the GC base pair, the proton transfer follows pathway (1).

The situation becomes more complicated when the protonated positions are the cytosine moiety. For the structure $\text{G}-\text{H}^+\text{C}_{\text{O}2}$ with the lengthened hydrogen bonds $(\text{G})\text{N}_1-\text{H} \cdots \text{N}_3(\text{C})$ (3.332 Å) and $(\text{G})\text{N}_2-\text{H} \cdots \text{O}_2(\text{C})$ (3.880 Å),¹⁸ no proton transfer is found. For the structure $\text{G}-\text{H}^+\text{C}_{\text{C}2}$, the two moieties have a small charge difference (NBO charge 0.42 for guanine and 0.58 for cytosine). The H_1 proton of guanine transfers following the shortest $(\text{G})\text{N}_1-\text{H} \cdots \text{N}_3(\text{C})$ of the three hydrogen bonds and leaves the NBO charges redistributed in the product of the proton transfer, i.e., 0.12 on the guanine and 0.88 on the cytosine. For structure $\text{G}-\text{H}^+\text{C}_{\text{N}3}$, the NBO charges become 0.15 on the guanine and 0.85 on cytosine upon protonation. The hydrogen bond $(\text{G})\text{O}_6 \cdots \text{H}-\text{N}_3(\text{C})$ is much shorter than the analogous distance for the neutral GCH radical. In fact, the $\text{O}_6 \cdots \text{H}$ distance is so short (1.392 Å) that it might be considered a nearly covalent interaction. Thus the proton transfers from the N_3 site of cytosine to the O_6 site of guanine following the shorter hydrogen bond $(\text{G})\text{O}_6 \cdots \text{H}-\text{N}_3(\text{C})$. For the structures $\text{G}-\text{H}^+\text{C}_{\text{C}4}^{(1)}$ and $\text{G}-\text{H}^+\text{C}_{\text{C}6}$, the pathway of proton-transfer reaction still follows the N_1 site of guanine with the larger NBO charge (0.67 for guanine) to the N_3 site of cytosine with small NBO charge (0.33 for cytosine). The proton in the $\text{G}-\text{H}^+\text{C}_{\text{C}5}$ structure transfers from the N_4 site of cytosine to the O_6 site of guanine, i.e., the proton follows the shortest hydrogen bond $(\text{G})\text{O}_6 \cdots \text{H}-\text{N}_4(\text{C})$ and shifts from the high NBO charge distribution to the low NBO charge distribution.

3.3. Proton-Transfer Energy Profiles in the Gas and Solvent. Solvent effects can play a crucial role in highly polar systems and dramatically change the relative stability of various tautomers.^{28,44,55,56} Thus, we compute PCM single-point energies at the gas phase optimized structures (Figures 13 and 14). Apparently, the relative stabilities are enhanced significantly by bulk water (beyond 50 kcal/mol). The proton-transfer energy barrier is determined as the energy difference between the transition state and the appropriate conventional protonated GC.

The predicted energy barriers for proton transfer ($\text{GC}+\text{H}$)⁺ span in the range 0.2 to 6.5 kcal/mol in the gas phase and 0.6 to 10.3 kcal/mol in the solvent.

In general, when the proton is added to guanine moiety, the proton-transfer energy barriers are higher than those structures in which the proton is added to cytosine in the gas phase. The energies of the conventional protonated structures with the proton adding to the guanine moiety are lower than their proton-transferred products in the gas phase, except for $\text{H}^+\text{G}_{\text{C}2}\text{-C}$ (Figure 13). For structure $\text{H}^+\text{G}_{\text{C}2}\text{-C}$, the proton-transfer process is a slightly exothermic reaction with a difference energy of 1 kcal/mol between the proton-transferred product $\text{H}^+\text{G}_{\text{C}2}\text{(-H}^+)\text{-C(+H}^+)\text{}_{\text{PT}}$ and the conventional protonated $\text{H}^+\text{G}_{\text{C}2}\text{-C}$. However for the other proton-transfer processes, when the protonated guanine site is far away from the internal hydrogen bonds, the higher energy barriers and even more disfavored proton-transferred products prevent the proton transfer. Therefore, the guanine-centered positive charge cation ($\text{GC}+\text{H}$)⁺ is generally lower in energy than the systems with positive charge centered on the cytosine moiety, in agreement with a previous theoretical study.¹⁸

However, the unfavorable charge separated proton transfer in the gas phase can be shielded in the aqueous phase by the water solvent. Although the energy barriers increase slightly, solvent effects greatly strengthen the stabilities of the products of the proton-transferred structures (Figure 13). Thus, solvent effects make the proton process even more favorable. The structure $\text{H}^+\text{G}_{\text{O}6}\text{-C}$ is a stark example for which $\text{H}^+\text{G}_{\text{O}6}\text{(-H}^+)\text{-C(+H}^+)\text{}_{\text{PT}}$ becomes more favorable in solution than $\text{H}^+\text{G}_{\text{O}6}\text{-C}$ by 1.8 kcal/mol, and the energy barrier for the reaction decreases to 3.4 kcal/mol, agreeing with Noguera's results.²⁸ Nevertheless, solvent effects have little effect on the proton-transfer reaction of structure $\text{H}^+\text{G}_{\text{N}7}\text{-C}$, which has the lowest energy in the gas phase.

Contrary to the guanine protonation, the proton-transferred products are more favorable than the conventional protonated structures when the protonation position is located on the cytosine in the gas phase, except for $\text{G-H}^+\text{C}_{\text{C}6}$ (Figure 14). For the structures $\text{G-H}^+\text{C}_{\text{N}3}$, $\text{G-H}^+\text{C}_{\text{C}5}$, and $\text{G-H}^+\text{C}_{\text{C}6}$, possessing lower relative energies, proton-transfer reactions become more difficult in solution because of the increased energy barriers and higher energies than the corresponding nonproton-transferred structures. For the highest energy structures $\text{G-H}^+\text{C}_{\text{C}2}$ and $\text{G-H}^+\text{C}_{\text{C}4}$ ⁽¹⁾, solvent effects have little effect on the proton transfer, similar to the case for structure $\text{H}^+\text{G}_{\text{N}7}\text{-C}$.

By consideration of the double-helix structure of the DNA sequence in solvent, we can get some rules from the 12 isomers' energy profiles in solvent on the different proton addition site from Figure 13 and 14. First, the structures in which proton added on the minor groove side (sites C_2 , N_3 , and C_4 in guanine and C_2 in cytosine) of the GC base pair prefer to proton transfer more easily than those protonated on major groove, and the energies of the proton-transferred products are lower than the corresponding conventional protonated structures. Second, the structures when the proton is added on the sites adjoining the hydrogen bonds ($\text{G}_{\text{C}2}$, $\text{G}_{\text{O}6}$, $\text{C}_{\text{C}2}$, and $\text{C}_{\text{C}4}$ sites) is easier to proton transfer than those protonated sites remote from the hydrogen bonds addition. The proton-transfer reaction of structure $\text{G-H}^+\text{C}_{\text{N}3}$ is unfavored energetically in solvent because the influence of charge different being shielded in the aqueous phase and the higher proton affinity of site $\text{C}_{\text{N}3}$ than that of site $\text{G}_{\text{O}6}$.

4. CONCLUSIONS

In general, the bond lengths of protonated GC structures, especially hydrogen bond lengths, change largely in the process of single proton transfer and ultimately lead to geometrical perturbations. Structures $\text{G}(\text{-H}^+)\text{-H}^+\text{C}_{\text{C}2}\text{(+H}^+)\text{}_{\text{PT}}$ and $\text{G}(\text{+H}^+)\text{-H}^+\text{C}_{\text{C}4}\text{(-H}^+)\text{}_{\text{PT}}$ ⁽²⁾, with significant twist, might cause DNA damage due to proton transfer. The $\text{H}^+\text{G}_{\text{O}6}\text{(-H}^+)\text{-C(+H}^+)\text{}_{\text{TS}}$ structure loses the C_s symmetry of its conventional protonated structure.

For the proton-transfer processes in the protonated GC base pairs, three proton-transfer pathways are found. The first pathway is H_1 proton transfer from site N_1 of guanine to the N_3 site of cytosine; the second pathway involves H_{4a} proton transfer from N_4 of cytosine to the O_6 site of guanine, and the third pathway is H_{2a} proton transfer from site N_2 of guanine to the O_2 site of cytosine. The first proton-transfer path is viable when the proton adds to the guanine (see Figures 1–7). During these proton-transfer processes, the energy barriers are small and the positive charge distribution center of guanine shifts to the cytosine. When the proton is attached to the C_4 or C_6 position of cytosine, the "positive charge" remains at the guanine moiety, H_1 transfers from the N_1 site of guanine to the N_3 site of cytosine. When a proton is attached to the C_2 site of cytosine, the charge distributions on guanine and cytosine have small differences due to the H_{2a} transferred from the N_2 site of guanine to the O_2 site of cytosine forming the conventional protonated GC base pair. Thus, the second H_1 transfer follows the shortest hydrogen bond, i.e., the first path is observed. When protonation located on site C_5 of cytosine occurs, inducing the positive charge center distributed on cytosine, the second proton-transfer path is found for the structure $\text{G-H}^+\text{C}_{\text{C}5}$. The third proton-transfer pathway is found only for structure $\text{G-H}^+\text{C}_{\text{C}4}$, in which the H_{2a} proton oscillates between the N_2 site of guanine and the O_2 site of cytosine, because the proton-transferred product $\text{G}(\text{-H}^+)\text{-H}^+\text{C}_{\text{C}4}\text{(+H}^+)\text{}_{\text{PT}}$ ⁽³⁾ and corresponding conventional protonated structure have essentially the same energy. For the structure $\text{G-H}^+\text{C}_{\text{N}3}$, in which only two hydrogen bonds are formed, the attached H_3 proton transfers from the N_3 site of cytosine to guanine O_6 . No proton transfer is found for the $\text{G-H}^+\text{C}_{\text{O}2}$ structure because of the longer hydrogen bonds between the guanine and cytosine moieties.

In the gas phase, the proton-transfer profiles show that if the proton is attached to the six-centered sites adjoining the hydrogen bonds, such as the sites $\text{G}_{\text{C}2}$, $\text{C}_{\text{C}2}$, $\text{C}_{\text{N}3}$, and $\text{C}_{\text{C}4}$, the conventional protonated structures are unclear. Therefore, such proton transfers are prone to take place, and the proton-transferred product structures lie lower in energy than the corresponding conventional protonated structures. If the proton is attached to a site remote from the hydrogen bonds, the structures with the positive charge distribution on guanine are much more favorable than those with the positive charge primarily on cytosine. In aqueous solution, the stabilities of various tautomers are enhanced significantly. The charge difference resulting in proton transfer in the gas phase can be shielded by the water solvent. The proton added on the minor groove and the sites adjoining the hydrogen bonds are favored of the proton-transfer reaction.

■ AUTHOR INFORMATION

Corresponding Author

*E-mail: yuxialin@163.com.

■ ACKNOWLEDGMENT

We are grateful to the China National Science Foundation (Grant No. 10974161) and the Sichuan Province Youth Science and Technology Foundation (2008-20-360) for support of this work. This research was also supported by U.S. National Science Foundation, Grant No. CHE-1054286.

■ REFERENCES

- (1) Watson, J. D.; Crick, F. H. C. *Nature* **1953**, *171*, 737–738.
- (2) Hariharan, P. C.; Pople, J. A. *Theor. Chim. Acta* **1973**, *28*, 213–222.
- (3) Leś, A.; Adamowicz, L. *J. Phys. Chem.* **1989**, *93*, 7078–7081.
- (4) Colominas, C.; Luque, F. J.; Orozco, M. *J. Am. Chem. Soc.* **1996**, *118*, 6811–6821.
- (5) Hutter, M.; Clark, T. *J. Am. Chem. Soc.* **1996**, *118*, 7574–7577.
- (6) Colson, A. O.; Besler, B.; Sevilla, M. D. *J. Phys. Chem.* **1993**, *97*, 13852–13859.
- (7) Sevilla, M. D.; Besler, B.; Colson, A. O. *J. Phys. Chem.* **1995**, *99*, 1060–1063.
- (8) Hush, N. S.; Cheung, A. S. *Chem. Phys. Lett.* **1975**, *34*, 11–13.
- (9) Orlov, V. M.; Smirnov, A. N.; Varshavsky, Y. M. *Tetrahedron Lett.* **1976**, *48*, 4377–4378.
- (10) Smets, J.; Houben, L.; Schoone, K.; Maes, G.; Adamowicz, L. *Chem. Phys. Lett.* **1996**, *262*, 789–796.
- (11) Ha, T.-K.; Keller, H.-J.; Gunde, R.; Gunthard, H.-H. *J. Phys. Chem. A* **1999**, *103*, 6612–6623.
- (12) Chandra, A. K.; Nguyen, M. T.; Uchimaru, T.; Zeegers-Huyskens, T. *J. Phys. Chem. A* **1999**, *103*, 8853–8860.
- (13) Podolyan, Y.; Gorb, L.; Leszczynski, J. *J. Phys. Chem. A* **2000**, *104*, 7346–7352.
- (14) Noguera, M.; Rodríguez-Santiago, L.; Sodupe, M.; Bertran, J. *J. Mol. Str.* **2001**, *537*, 307–318.
- (15) Kampf, G.; Kapinos, L. E.; Griesser, R.; Lippert, B.; Sigel, H. *J. Chem. Soc., Perkin Trans. 2* **2002**, *2*, 1320–1327.
- (16) Gu, J. D.; Wang, J.; Leszczynski, J. *J. Am. Chem. Soc.* **2004**, *126*, 12651–12660.
- (17) Zhang, J. D.; Schaefer, H. F. *J. Chem. Theory Comput.* **2007**, *3*, 115–126.
- (18) Wang, H. Y.; Zhang, J. D.; Schaefer, H. F. *ChemPhysChem* **2010**, *11*, 622–629.
- (19) Lyngdoh, R. H. D.; Schaefer, H. F. *Acc. Chem. Res.* **2009**, *42*, 563–572.
- (20) Löwdin, P.-O. *Rev. Mod. Phys.* **1963**, *35*, 724–732.
- (21) Löwdin, P.-O. *Adv. Quantum Chem.* **1965**, *2*, 213–361.
- (22) Kong, Y. S.; Jhon, M. S.; Löwdin, P.-O. *Int. J. Quantum Chem. Symp.* **1987**, *14*, 189.
- (23) Florián, J.; Leszczynski, J. *J. Am. Chem. Soc.* **1996**, *118*, 3010–3017.
- (24) Cerón-Carrasco, J. P.; Requena, A.; Perpète, E. A.; Michaux, C.; Jacquemin, D. *Chem. Phys. Lett.* **2009**, *484*, 64–68.
- (25) Bertrand, P. *Radiat. Phys. Chem.* **2005**, *72*, 105–110.
- (26) Gorb, L.; Podolyan, Y.; Dziekonski, P.; Sokalski, W. A.; Leszczynski, J. *J. Am. Chem. Soc.* **2004**, *126*, 10119–10129.
- (27) Florián, J.; Hrouda, V.; Hobza, P. *J. Am. Chem. Soc.* **1994**, *116*, 1457–1460.
- (28) Noguera, M.; Sodupe, M.; Bertrán, J. *Theor. Chem. Acc.* **2004**, *112*, 318–326.
- (29) Noguera, M.; Sodupe, M.; Bertrán, J. *Theor. Chem. Acc.* **2007**, *118*, 113–121.
- (30) Hrouda, V.; Florián, J.; Polášek, M.; Hobza, P. *J. Phys. Chem.* **1994**, *98*, 4742–4747.
- (31) Cerón-Carrasco, J. P.; Requena, A.; Michaux, C.; Perpète, E. A.; Jacquemin, D. *J. Phys. Chem. A* **2009**, *113*, 7892–7898.
- (32) Cerón-Carrasco, J. P.; Requena, A.; Zúñiga, J.; Michaux, C.; Perpète, E. A.; Jacquemin, D. *J. Phys. Chem. A* **2009**, *113*, 10549–10556.
- (33) Colson, A. O.; Besler, B.; Close, D. M.; Sevilla, M. D. *J. Phys. Chem.* **1992**, *96*, 661–668.
- (34) Colson, A. O.; Besler, B.; Sevilla, M. D. *J. Phys. Chem.* **1992**, *96*, 9787–9794.
- (35) Bertran, J.; Oliva, A.; Rodriguez-Santiago, L.; Sodupe, M. *J. Am. Chem. Soc.* **1998**, *120*, 8159–8167.
- (36) Li, X. F.; Cai, Z. L.; Sevilla, M. D. *J. Phys. Chem. B* **2001**, *105*, 10115–10123.
- (37) Pulkkinen, S.; Noguera, M.; Rodríguez-Santiago, L.; Sodupe, M.; Bertran, J. *Chem.—Eur. J.* **2000**, *6*, 4393–4399.
- (38) Noguera, M.; Bertran, J.; Sodupe, M. *J. Phys. Chem. A* **2004**, *108*, 333–341.
- (39) Noguera, M.; Bertrán, J.; Sodupe, M. *J. Phys. Chem. B* **2008**, *112*, 4817–4825.
- (40) Nonin, S.; Leroy, J.-L.; Guérion, M. *Nucl. Acid Res.* **1996**, *24*, 586–595.
- (41) Kumar, A.; Sevilla, M. D. *J. Phys. Chem. B* **2009**, *113*, 11359–11361.
- (42) Adhikary, A.; Khanduri, D.; Sevilla, M. D. *J. Am. Chem. Soc.* **2009**, *131*, 8614–8619.
- (43) Chen, H. Y.; Yeh, S. W.; Hsu, S. C. H.; Kao, C. L.; Dong, T. Y. *Phys. Chem. Chem. Phys.* **2011**, *13*, 2674–2681.
- (44) Cerón-Carrasco, J. P.; Zúñiga, J.; Requena, A.; Perpète, E. A.; Michaux, C.; Jacquemin, D. *Phys. Chem. Chem. Phys.* **2011**, *13*, 14584–14589.
- (45) Becke, A. D. *J. Chem. Phys.* **1993**, *98*, 5648–5652.
- (46) Lee, C.; Yang, W.; Parr, R. G. *Phys. Rev. B* **1988**, *37*, 785–789.
- (47) Latajka, Z.; Bouteiller, Y. *J. Chem. Phys.* **1994**, *101*, 9793–9799.
- (48) Lee, C.; Fitzgerald, G.; Planas, M.; Novoa, J. *J. J. Phys. Chem.* **1996**, *100*, 7398–7404.
- (49) Frisch, M. J.; Trucks, G. W.; Schlegel, H. B.; Scuseria, G. E.; Robb, M. A.; Cheeseman, J. R.; Montgomery, J. A., Jr.; Vreven, T.; Kudin, K. N.; Burant, J. C.; Millam, J. M.; Iyengar, S. S.; Tomasi, J.; Barone, V.; Mennucci, B.; Cossi, M.; Scalmani, G.; Rega, N.; Petersson, G. A.; Nakatsuji, H.; Hada, M.; Ehara, M.; Toyota, K.; Fukuda, R.; Hasegawa, J.; Ishida, M.; Nakajima, T.; Honda, Y.; Kitao, O.; Nakai, H.; Klene, M.; Li, X.; Knox, J. E.; Hratchian, H. P.; Cross, J. B.; Bakken, V.; Adamo, C.; Jaramillo, J.; Gomperts, R.; Stratmann, R. E.; Yazyev, O.; Austin, A. J.; Cammi, R.; Pomelli, C.; Ochterski, J. W.; Ayala, P. Y.; Morokuma, K.; Voth, G. A.; Salvador, P.; Dannenberg, J. J.; Zakrzewski, V. G.; Dapprich, S.; Daniels, A. D.; Strain, M. C.; Farkas, O.; Malick, D. K.; Rabuck, A. D.; Raghavachari, K.; Foresman, J. B.; Ortiz, J. V.; Cui, Q.; Baboul, A. G.; Clifford, S.; Cioslowski, J.; Stefanov, B. B.; Liu, G.; Liashenko, A.; Piskorz, P.; Komaromi, I.; Martin, R. L.; Fox, D. J.; Keith, T.; Al-Laham, M. A.; Peng, C. Y.; Nanayakkara, A.; Challacombe, M.; Gill, P. M. W.; Johnson, B.; Chen, W.; Wong, M. W.; Gonzalez, C.; Pople, J. A. *Gaussian 09*, revision A.1; Gaussian, Inc.: Wallingford, CT, 2004.
- (50) Huzinaga, S. *J. Chem. Phys.* **1965**, *42*, 1293–1302.
- (51) Dunning, T. H. *J. Chem. Phys.* **1970**, *53*, 2823–2833.
- (52) Lee, T. J.; Schaefer, H. F. *J. Chem. Phys.* **1985**, *83*, 1784–1794.
- (53) Rienstra-Kiracofe, J. C.; Tschumper, G. S.; Schaefer, H. F.; Nandi, S.; Ellison, G. B. *Chem. Rev.* **2002**, *102*, 231–282.
- (54) Zhang, J. D.; Chen, Z. F.; Schaefer, H. F. *J. Phys. Chem. A* **2008**, *112*, 6217–6226.
- (55) Hanus, M.; Ryjáček, F.; Kabeláč, M.; Kubář, T.; Bogdan, T. V.; Trygubenko, S. A.; Hobza, P. *J. Am. Chem. Soc.* **2003**, *125*, 7678–7688.
- (56) Jang, Y. H.; Goddard, W. A.; Noyes, K. T.; Sowers, L. C.; Hwang, S.; Chung, D. S. *J. Phys. Chem. B* **2003**, *107*, 344–357.